https://doi.org/10.34883/PI.2024.13.2.009

Heal H.H.[1]✉, Al-Dallee Z.T.[1], Khadam E.J.[2]
[1] University of Basrah, Basrah, Iraq
[2] University of Baghdad, Baghdad, Iraq

Antibacterial and Cytotoxic Properties of Silver Nanoparticles with Luteolin: Technology of Their Synthesis and Characteristics

Conflict of interest: nothing to declare.
Authors' contribution: Heal H.H. – conceptualization, methodology, investigation, resources, data curation, writing – original draft, soft wire; Al-Dallee Z.T. – supervision, conceptualization, methodology, formal analysis, investigation; Khadam E.J. – supervision, conceptualization, methodology, writing – original draft.
The article is published in the author's edition.

Submitted: 02.09.2023
Accepted: 22.04.2024
Contacts: medicalresearch77@yahoo.com

Abstract

Introduction. Every industry, including health, nutrition, and energy, has been revolutionized by the advent of nanoparticles (NPs). There are several advantages to using nanotechnology in medicine, particularly for medication delivery. In order to create diverse metal nanocomposites with antibacterial and anticancer capabilities, green metal nanoparticle synthesis has been shown to be an efficient and environmentally friendly method.
Purpose. Synthesis luteolin silver nanoparticles (LuAgNPs) then characterization, test antibacterial and cytotoxicity.
Materials and methods. Luteolin used as reducing agent for synthesis LuAgNPs after addition to agno3 solution then undergo characterization. The antibacterial properties of LuAgNPs against gram bacteria (+) and gram (–) bacteria are studied. The cytotoxic effect of LuAgNPs and luteolin was also studied using the Microculture tetrazolium assays (MTT) assay method against cell lines MCF-7.
Results. Best parameter for LuAgNPs synthesis was PH=7, T=70 °. It has been shown that LuAgNPs have more antibacterial effect for gram-negative bacteria than gram positive bacteria. Luteolin silver nanoparticles showed high cytotoxic activity for luteolin silver nanoparticles than for luteolin.
Conclusion. Luteolin silver nanoparticles shows promising antibacterial activity against both Gram-positive and Gram-negative bacteria. Luteolin silver nanoparticles have significant anticancer activity.
Keywords: anticancer activity, nanostructure, X-ray diffraction (XRD), microculture tetrazolium assays, green metal nanoparticle

Хеаль Х.Х.[1]✉, Аль-Далли З.Т.[1], Хадам Э.Дж.[2]
[1] Университет Басры, Басра, Ирак
[2] Университет Багдада, Багдад, Ирак

Антибактериальные и цитотоксические свойства наночастиц серебра с лютеолином: технология их синтеза и характеристика

Конфликт интересов: не заявлен.
Вклад авторов: Хеаль Х.Х. – концепция, методология, проведение исследований, ресурсы, обработка данных, написание исходного текста статьи, программное обеспечение; Аль-Далли З.Т. – научное руководство, концепция, методология, анализ данных, проведение исследований; Хадам Э.Дж. – научное руководство, концепция, методология, написание исходного текста статьи.
Статья опубликована в авторской редакции.

Подана: 02.09.2023
Принята: 22.04.2024
Контакты: medicalresearch77@yahoo.com

Резюме

Введение. Наночастицы (НЧ) произвели революцию во всех отраслях экономики, включая здравоохранение, производство продуктов питания и энергетику. Использование нанотехнологий в медицине, в частности для доставки лекарственных препаратов, имеет ряд преимуществ. Для создания разнообразных нанокомпозитных соединений металлов с антибактериальными и противораковыми свойствами был разработан эффективный и экологически чистый метод «зеленого» синтеза наночастиц металлов.
Цель. Синтез наночастиц серебра с лютеолином (LuAgNPs), их характеристики, исследование антибактериальных и цитотоксических свойств.
Материалы и методы. Лютеолин использовали в качестве восстанавливающего агента при синтезе LuAgNPs после добавления к раствору $AgNO_3$, затем анализировали характеристики полученного вещества. Исследованы антибактериальные свойства LuAgNPs в отношении грамположительных (+) и грамотрицательных (–) бактерий. Кроме того, определено цитотоксическое действие LuAgNPs и лютеолина на клеточной линии MCF-7 с помощью микрокультурного тетразолиевого теста (MTT).
Результаты. Оптимальными условиями для синтеза LuAgNPs были pH=7 и t=70 °C. Установлено, что LuAgNPs обладают более выраженным антибактериальным действием в отношении грамотрицательных бактерий, чем в отношении грамположительных. Наночастицы серебра с лютеолином проявляли более выраженную цитотоксическую активность к наночастицам серебра с лютеолином, чем к лютеолину.
Заключение. Определение антибактериальной активности наночастиц серебра с лютеолином в отношении как грамположительных, так и грамотрицательных бактерий представляется весьма перспективным, тем более что наночастицы серебра с лютеолином демонстрируют выраженную противоопухолевую активность.
Ключевые слова: противоопухолевая активность, наноструктура, рентгеновская дифракция (XRD), микрокультурный тетразолиевый тест, «зеленая» металлическая наночастица

■ INTRODUCTION

Nanotechnology is a growing field and can be utilized to build tiny structures [1]. The Greek term for dwarf is the source of the word "nano", which refers to one billionth of substance [2]. It is one of the sectors of biotechnology that is developing and has a wide range of applications [3]. The ability to discern between different types of nanoscale compounds creates a variety of applications as well as prospects for new scientific study [4]. Pharmaceuticals tailored medication delivery methods, inhibitory agents for biofilm development, are just a few of the businesses that nanoparticle employ it [5].

AgNPs are useful as antibacterial agents, medication delivery vehicles, and physical therapy tools in the medical profession They may cause DNA damage, cytokine production, cell death through apoptosis, oxidative stress, and mitochondrial membrane changes [6]. Antibacterial nanoparticles are primarily used in the medical industry to create dressings, coatings, and systems for drug because they provide a solution to the increasing antibiotic resistance of bacteria [7]. Silver nanoparticles (AgNPs) are recently shown to have stronger antibacterial properties than basic silver [8] green synthesis which focuses on the development of cleaner, lower-temperature procedures and the use of natural extracts, especially those packed with polyphenolic substance – emerged with the help of environmentally friendly techniques. The aromatic benzene rings in the polyphenolic product have their hydroxyl (-OH) groups swapped out. These hydroxyl groups aid in the reduction of reactive metallic ions, including Ag (silver) ions, to nanoparticles made of silver (AgNPs) [9].

There are several research projects that use plant extracts high in flavonoids to create silver nanoparticles. In this work, flavonoids are used to try to create silver nanoparticles directly as opposed to plant extracts high in flavonoids. Vitex pseudo negundo's luteolin was isolated, extracted, and utilized to create LuAgNPs nanoparticles.

■ PURPOSE OF THE STUDY

Synthesis luteolin silver nanoparticles (LuAgNPs) then characterization, test antibacterial and cytotoxicity.

■ MATERIALS AND METHODS

Materials

Material used in this study were listed in table 1.

Table 1
Chemicals and materials used

Material	Supplier	Company
Molar Hinton agar	Capricorn	Germany
DMSO	Loba chemie	India
Luteolin	Medochiem	China
MTT	Bio-World	USA
RPMI -1640	Medochiem	China
Molar Hinton agar	Capricorn	Germany
Fetal bovine serum	Capricorn	Germany
Sliver nitrate (AgNO3)	Himedia	India

Methods

luteolin Silver Nanoparticle Synthesis

After making minor adjustments, [10] used the flavonoid luteolin to chemically reduce a salt solution of silver nitrate to create silver nanoparticles.

Aqueous Silver nitrate Preparation

1 mM aqueous solution of silver nitrate (AgNO3) was made by combining 0.00425 g of AgNO3 with 25 mL of deionized water; this mixture was stirred constantly until the clear off-white solution showed.

Luteolin Solution Preparation

Preparing 2 mM Solution of luteolin was done by mixing 0.0025 g of luteolin, with 10 mL of a mixture of methanol (99.8%) and distilled water (1:1 water-alcohol mixture), and the to guarantee that there are no remaining particles in the solution, the mixture was sonicated for five min.

Formation of Luteolin-Loaded Silver Nanoparticles

In order to ensure proper synthesis of the LuAgNPs, the luteolin liquid system was combined with the Mixture of silver nitrate at a ratio of (1:9 and 2:8) and maintained on a magnetic stirrer at 400 rpm for 10–30 min. The mixture was then allowed to rest for 24 h while being shielded from light. The color of the solution was changed slowly form pale yellowish to dark brown depicted the synthesis of silver nanoparticles. It was necessary to measure the spectra of absorption at periods of 10, 20, and 30 minis to establish the ideal amount of time for completely reducing AgNO3. The reaction was carried out at temperatures of 40 and 70 °C to ascertain the impact of temperature on the synthesis of LuAgNPs. To assess the effect of pH on the synthesis of LuAgNPs, the reaction was carried out at various pH (6, 8 and 7) that were changed using 0.1 N NaOH and 0.1 N HNO3. After the synthesis of LuAgNPs, the suspensions were centrifuged at 12 000 rpm for 10 min. Residue was collected, washed with deionized water, and dried in a drying oven for 24 h at 40 °C, and stored at 20 °C for characterizations and further biological activity application.

Luteolin Silver Nanoparticles Characterization

Change of Color

With the naked eye, the solution's hue changed from yellow to dark brown, signifying the bio-reduction of silver nitrate to LuAgNPs [11].

Ultra-Violate Visible Spectroscopy (UV-Vis)

With a wavelength range between 200 and 800 nm, the CECIL7200 UV-visible spectrophotometer was used to monitor the early characterizations of silver nanoparticles. As the blank, luteolin solution was used.

Fourier Transform Infrared Spectroscopy (FTIR)

After centrifuging, collecting, washing, and drying the powdered sample from the prepared solution of LuAgNPs, it was analyzed using Fourier Transform Infrared (FTIR) spectra in order to the groups of molecules in charge of the reducing of silver ions should

be identified. With aid of KBr disc (Shimadzu/84005 at IRAN -Tehran in Tehran university) FTIR analysis was done. The range of the absorbance was 4000 to 500 cm1 [12].

Dynamic Light Scattering (DLS)

HORIBA SZ-100 for Windows [Z Type] Ver2. 20 was used in conjunction with the Dynamic Light Scattering (DLS) technique to validate the LuAgNPs' size. The experiments were carried out at room temperature using the the Lu AgNPs dry powder was diluted at a 1: 10 ratios with deionized water. The investigation was carried out in Tehran University, IRAN.

X-Ray Diffraction (XRD) Analysis

Using a Bruker 2010/D2Phaser, the crystallization of silver nanoparticles was characterized and examined using X-ray diffraction (XRD). The investigation was carried out in Tehran University, IRAN, using Cu K1 radiation (=1.540562 Ao) at 30 mA current and 40 kV voltages.

Scanning Electron Microscopy (SEM)

At the Tehran University in Iran, the shape of the produced nanoparticles was assessed using a scanning electron microscope (SEM, Germany).

Antibacterial Assay of Ag Nanoparticle

The well diffusion method was used to assess the antibacterial properties of LuAgNPs [13]. Gram-positive (Staphylococcus aureus, Streptococcus pneumonia) and Gram-negative (Escherichia coli, Pseudomonas aeruginosa) bacteria were used to evaluate the LuAgNPs. Bacterial isolates utilized in the experiment were provided by the microbiology lab at Basra University's Pharmacy College. The microbial strains were infused in nutritional broth and cultured for 24 h at a temperature of 35±2 °C. When compared to 0.5 McFarland mixture, which represent 1–2 108 colony forming units (CFU/mL), the turbidity of the culture broths was measured. As a solid growth medium, the medium was evenly placed on Mueller-Hinton agar plates using a sterile swab. To make a well on the surface of the inoculated plate, a sterilized cork borer was used. After diluting silver nanoparticles with DMSO and adding 20 µl of each particle concentration (100, 250, and 500 µg/ml) to each pore, the infected plate was pounded with a sterilized cork borer to create a well on the surface. Following that, the plates were left to incubate for 18 to 24 hat 37 °C. measuring the inhibition zones in (mm) used to determine the silver nanoparticles' ability to prevent the growth of the tested microorganisms.

Anti-cancer Assay of Luteolin Silver Nanoparticles

The work done at Gama tech company, Al-Hillah, Iraq.

Cell lines

To test the anti-tumor effects of luteolin and LuAgNPs, breast cancer cell lines were employed (MCF-7).

Growth Media and Culture Conditions

In addition to ten percent foetal bovine serum (BS) and antibiotic doses of 100 unit/ml of penicillin and 0.1 mg/ml of streptomycin, all cell lines were suspended in RPMI

1640 media. Cells line were cultured at 37 °C with 5% CO2 supply in a humidified incubator (Cypress Diagnostics).

Anti-tumor Assay Method

MTT assay method [14] was used to determine the antitumor activity of luteolin isolated from Vitex pseudonegundo grown in Iraq and LuAgNPs. Using 96-well plates for seeding, MCF-7 cell lines were dispersed into 1 ×104 cells/well. Cells were exposed to increasing concentrations of luteolin, LuAgNPs (6.25 µg/mL, 12.5 µg/mL, 25 µg/mL, 50 µg/mL, 100 µg/mL, 200 µg/mL) after forming a monolayer or incubating for 24 h. 75 h of incubation were followed by the addition of 28 L of a 0.002% w/v MTT solution, and cells were then incubated at 37 °C for 2.5 h before the MTT solution was withdrawn, the remaining crystals in the well were dissolved in 130 µL of dimethyl Sulphoxide, then 15 min of shaking incubation at 37 °C. Using a microplate reader with a 492 nm wave length, the ability to absorb was assessed. There were three runs of the assay. The results of three replicate measurements were provided as mean ±SEM. IC50 values of luteolin and LuAgNPs were computed after 24 h of treatment using Graph Pad Prism 6 and an inverted microscope to detect the morphological changes to the cell. The cell was seeded onto a 24-well plate and incubated for one day at 37 °C. Crystal violates was used to stain the cells, and after 15 min of incubation stain was washed with water and the cells were examined at 100 times their original size. The percentage of viable cells in each treatment concentration was computed as a ratio of sample to control.

Statistical Analysis

SPSS (statistical package for social science) was used to do the data analysis. The chi-square test, version 240, was used for evaluating means at the $p \leq 0.05$ of significance.

■ RESULTS AND DISCUSSION

Ag-nanoparticle Synthesis

The optimal conditions were selected according to the composition of the silver nanoparticle and found that it is as follows the volume of luteolin is 1 ml and the temperature is 70 °C and an acid function is equal to 7 and within a period of time not exceeding 10 min.

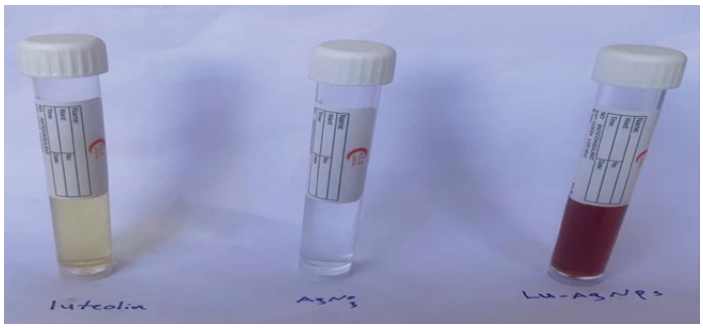

Fig. 1. Color change to Agno3 solution after addition of luteolin

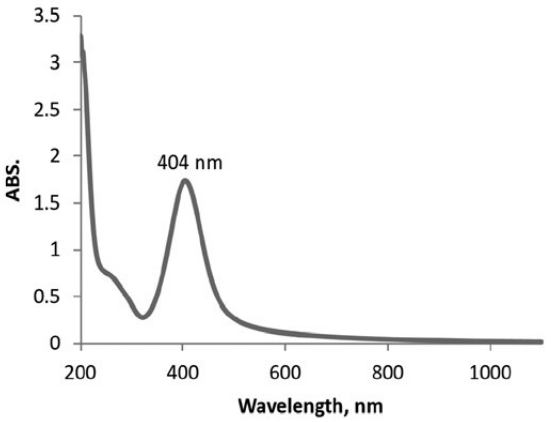

Fig. 2. UV-Visible spectra of luteolin silver nanoparticle show that maximum absorption at 404

Luteolin Silver Nanoparticles Characterization

UV-Visible Spectroscopy

UV-Vis spectroscopy is an essential tool for monitoring the electrical structure and spectral characteristics of the produced nanoparticles (NPs) for observing the production of LuAgNPs [15]. As seen in (Fig. 2), the highest silver nanoparticle concentration at roughly 404 nm caused a reaction to turn brown due to a Plasmon resonance peak. LuAgNPs' UV spectrum was recorded from 10 min. to 24 h. of incubation. As a consequence, 24 h was chosen as the ideal incubation period for the production of AgNPs. localized surface plasmon excitation, emergence of a significant band in the spectral pattern is due to intense light scattering by a field of electricity at a wavelength where the resonance happens.

Fourier-Transform Infrared Spectra (FTIR)

In order to identify the probable functional groups of the biomolecules in the active extracts that may be responsible for the stability of the generated LuAgNPs and the reduction of silver ions, we employed FTIR spectroscopy [16]. At wavenumbers between 4000 and 500 cm1, luteolin and artificial LuAgNPs were compared. FTIR spectroscopy showed that photochemical analysis of aqueous luteolin, it shows prominent bands of absorbance of CH aliphatic at 3089 cm-1, OHstr at 3398 cm-1, C=Ostr at 1665 cm-1, C=C aromatic at 1613, 1571, 1506 cm-1, C=Ostr at 1665 cm-1, C-Ostr at 1262, 1304, 1205, 1159, and 1118 cm-1 t. The analysis of the FTIR spectra of the produced silver nanoparticles and aqueous luteolin (Fig. 3). The band changed from 3216 to 3348 cm-1 as a result of the vibrations caused by stretching of phenols and the OH of alcohols. The oxidation of alcohol to aldehyde during the reduction of Ag+ to Ag0 may be caused by the luteolin's -OH group. [17], The stretching vibration of C-H aliphatic hydrocarbons is responsible for the 3089 to 2924.18 cm-1 band, 1665 to 1610. These peaks result from LuAgNPs attaching to amide substituent groups, which boosts LuAgNPs' stability. The stretching vibration of carbonyl (C=O) is responsible for this band [18], 1613 to 1516.10 cm-1 band is related to the stretching type of vibration of C=C. The primary phenolic hydroxyls responsible for

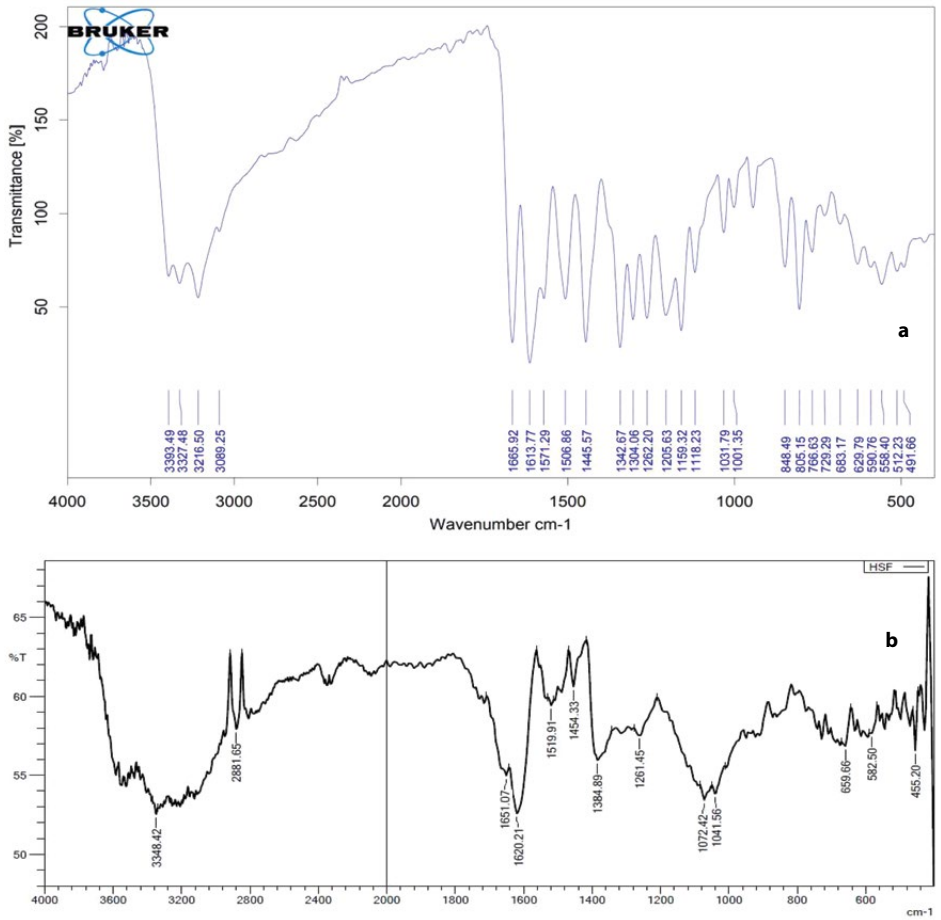

Fig. 3. FTIR spectra of (a) isolated luteolin, (b) luteolin silver nanoparticle

luteolin's key pharmacological activity and the molecular structure of luteolin have not changed, according to the FTIR and characterization investigations.

Dynamic Light Scattering (DLS)

DLS is based on the relationship between light and nanoparticles. It is possible to measure narrow size distribution with this approach, notably between 2 and 500 nm. To estimate the dispersed the light from a source of light travelling through the particles, it uses Rayleigh scattering method [19]. (Fig. 4) displays the hydrodynamic size distribution of LuAgNPs as calculated by DLS. 72 nm was found to be the average size of LuAgNPs. In this measurement, the Brown's motion theory for the dimension of particles is used. Brownian motion refers to the movement of the particles at arbitrarily in a gas or solutions. The average size of the nanoparticles was determined by examining the dynamic fluctuation of the light's scattering intensity and velocity of the motion of the particles in dispersion [20]. The LuAgNPs had polydispersity index (PDI) values of 0.541,

Table 2
Results of Calculations

Peak number	S.P Area Ratio	S. D	Mean	Mode
One	1.00	78.6 NM	37.0 NM	60.7 NM
Two	…	… NM	... NM	... NM
Three	…	… NM	… NM	... NM
Sum	1.0	78.6 NM	37.0 NM	60.7 NM

Table 3
Operations Cumulative

Zeta-Average	72.0 NM
Polydispersity index	0.541

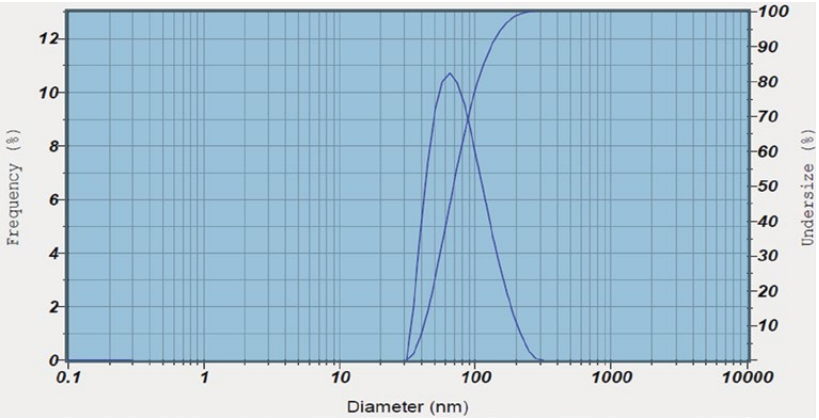

Fig. 4. DLS biosynthesized luteolin silver nanoparticle

which fall between 0 and 1, where 0 denotes monodisperse and 1 denotes polydisperse [20]. This outcome demonstrates unequivocally that the produced LuAgNPs were in a monodisperse phase and that there was little particle aggregation (table 2 and 3).

X-Ray Diffraction (XRD) Analysis

Crystallinity, isomorphous substitution, and particle size may all be determined using XRD (Fig. 5). Additionally, it has the ability to resolve different molecules and qualitatively identify active compounds [21]. When X-ray radiation reflects off of any particle, the number of diffraction peaks that are produced serves as a representation of the physicochemical characteristics of the crystalline lattice [22]. The crystal phase of the produced LuAgNPs was identified using XRD. The obtained LuAgNPs XRD spectra included the 20° to 80° range. 38.942° (110), 44.594° (199), 63.94° (220), and 76.89° (311) were the maxima at 2 values for AgNP-L. The maxima for AgNP-S can be seen in at 38.32° (111), 46.35° (200), 64.56° (220), and 77.40° (311). The identified peaks were compared to the silver library from that of the International Centre for Diffraction Data (ICDD) or the Joint Standing Committee on Powder Diffraction Standardization (JCPDS). On the synthesized LuAgNPs, four peaks were identified as 110, 199, 220, and 311; these peaks corresponded to the

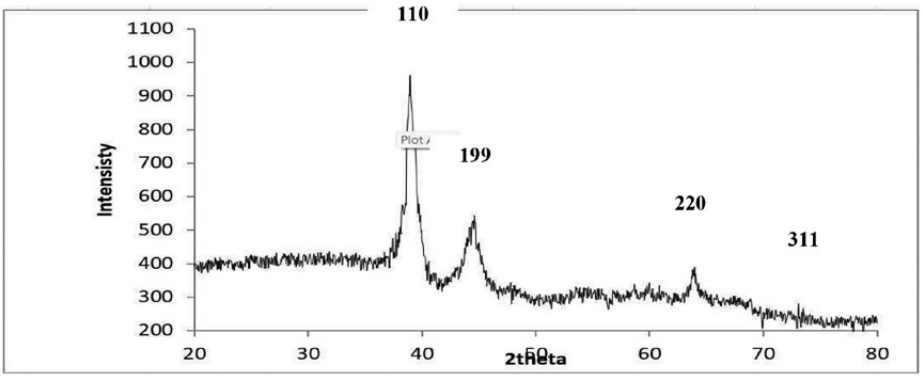

Fig. 5. XRD of the biosynthesized of LuAgNPs

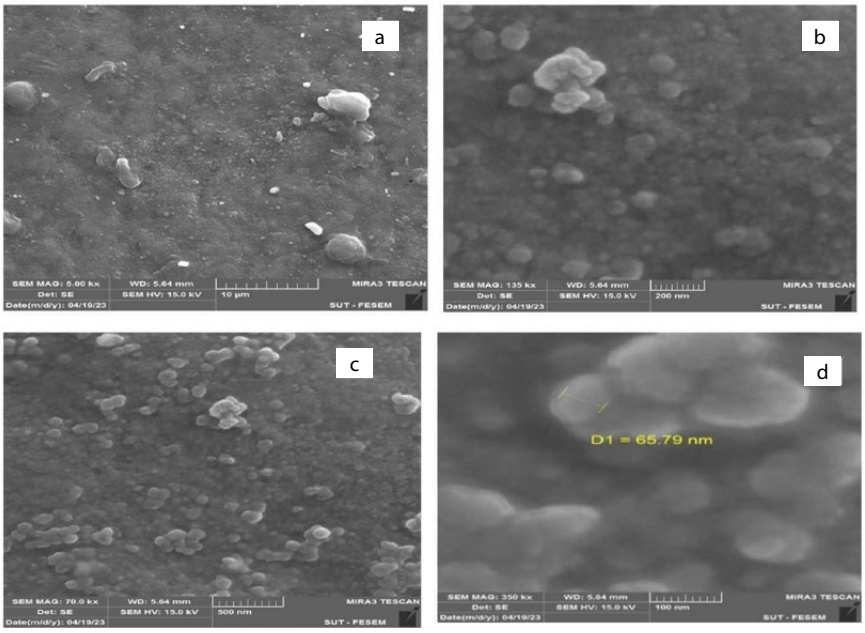

Fig. 6. SEM image of luteolin silver nanoparticle with magnifications: a – 5 kx; b – 70 kx; c – 135 kx; d – 350 kx

face-centered cubic (FCC) structure of silver (JCPDS file no. 04-0783) [23], and nearly same results were reported by [24].

Scanning Electron Microscopy (SEM)

SEM is a technique for capturing images of surfaces that has the ability to the ability to distinguish between distinct dimensions of particles, particle variability, nanoparticle structures, and the surface appearance of generated NPs at both microscopic and

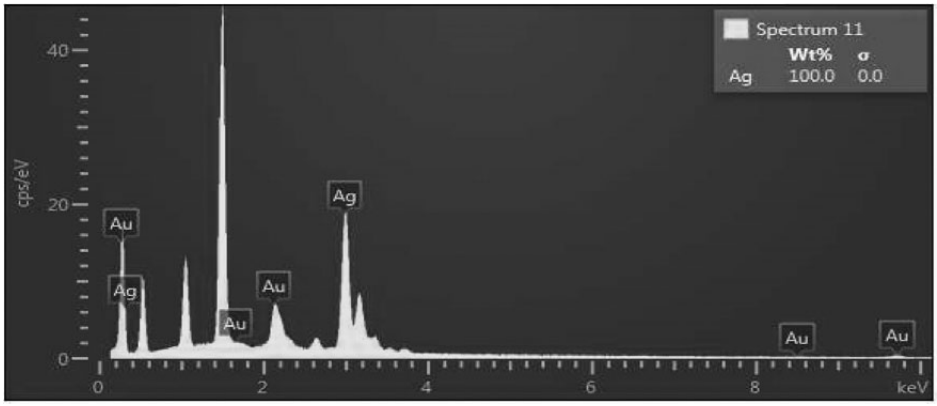

Fig. 7. EDX of luteolin silver nanoparticle

nanoscales [25]. The elements could be examined and the form of the silver nanoparticles could be evaluated using a combination of SEM and EDX. Depending on the SEM pictures (Fig. 6). The LuAgNPs were spherical and had rough surfaces. The larger LuAgNPs aggregates visible in the SEM picture were created as a result of the aggregation of smaller NPs. The synthesis of LuAgNPs was shown by the presence of white color dots in the photograph. Ag may be the primary element in LuAgNPs, according to the EDX spectra, which displayed a strong signal at 3 keV (Fig. 7).

Antibacterial Assay of Luteolin Silver Nanoparticles

Using the well diffusion method, the antibacterial activity of silver nanoparticles was investigated against pathogenic strains of gram-negative Escherichia coli, Pseudomonas aeruginosa, and gram-positive Streptococcus pneumoniae, as well as Staphylococcus aureus. supplied by the microbiology lab of Basra University's pharmacy college. Results of the inhibitory zones created by LuAgNPs' antibacterial activity are displayed in (table 4 and fig. 8). In contrast to Gram-negative bacteria, gram-positive bacteria have a thicker

Table 4
Anti bacrtial activity of LuAgNPs

Bactria	LuAgNPs conc (g/l)	Inhibition zone (mm)
Escherichia coli	100	25
	250	26
	500	28
Pseudomonas aeruginosa	100	23
	250	27
	500	29
Streptococcus pneumonia	100	20
	250	22
	500	24
Staphylococcus aureus	100	18
	250	23
	500	24

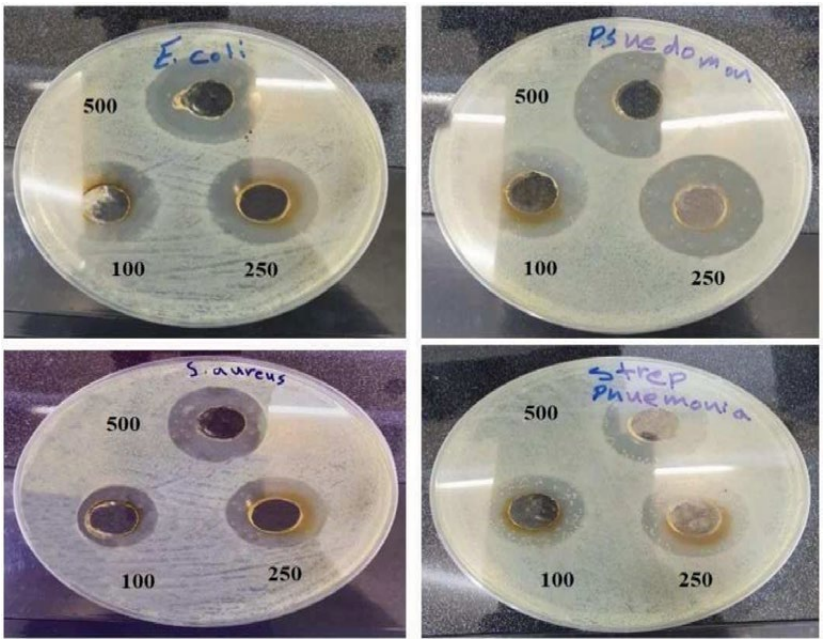

Fig. 8. Antibacterial assay of luteolin silver nanoparticle at different concentration (100, 250, 500 µg/ml)

peptidoglycan coating in their cell walls. Due to the characteristics of the peptidoglycan layer in Gram negative bacteria's cell walls, the biosynthesized LuAgNPs frequently demonstrate stronger antibacterial activities against these bacteria [26].

In-Vitro Cytotoxicity Assay of Luteolin Silver Nanoparticles

The IC50 values of the synthesised silver nanoparticles' anticancer activity in vitro against MCF-7 breast cancer cell lines were calculated using a chart of cell survival evaluated across a variety of concentrations among 1 and 100 g/mL after 24 h of exposure. MTT test, a colorimetric assay that measures the absorbance of a certain wave length in order to assess the anti-cancer activity of the medications or substances, is used to detect the correlation between cell activity and the number of viable cells [27]. The IC50 was calculated for luteolin, LuAgNPs, specifically at concentrations of 6.25, 12.5, 25, 50, 100, and 200 g/mL against the cell lines. This data's line chart generated an intersection between concentrations (X-axis) and percent inhibition (Y-axis) at 50% inhibition, which was then connected to the concentration value on the X-axis. The findings show that compared to normal luteolin, which had an average IC50 value of 59.59 g/ml, LuAgNPs had considerable cytotoxic action with an average IC50 value of 7.45 g/ml and significantly inhibited the proliferation of cancer cells (Fig. 9 and 10). The significant discrepancy between luteolin and LuAgNPs' IC50 And the the outcome demonstrated a significant difference below the threshold of significance of $p \leq 0.05$. (χ^2=0.00, df=8, p value =41.925). It is not difficult to imagine that the accessibility of a particle's surface area determines how it interacts with a cancer cell. Because of their higher surface area, smaller particles have more anticancer activity than bigger ones [28].

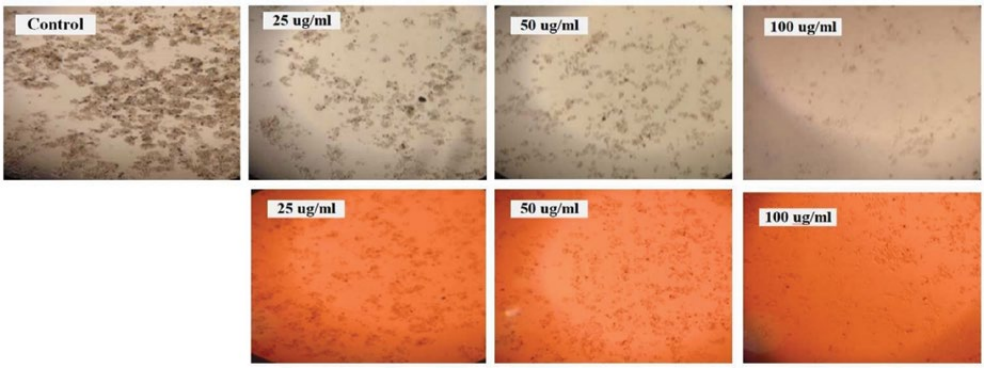

Fig. 9. Microscopic observations of the cytotoxic of AgNPs (in brown) and standard luteolin (in orange) on MFC-7 cell lines with different concentrations, control (untreated MFC-7 cell lines)

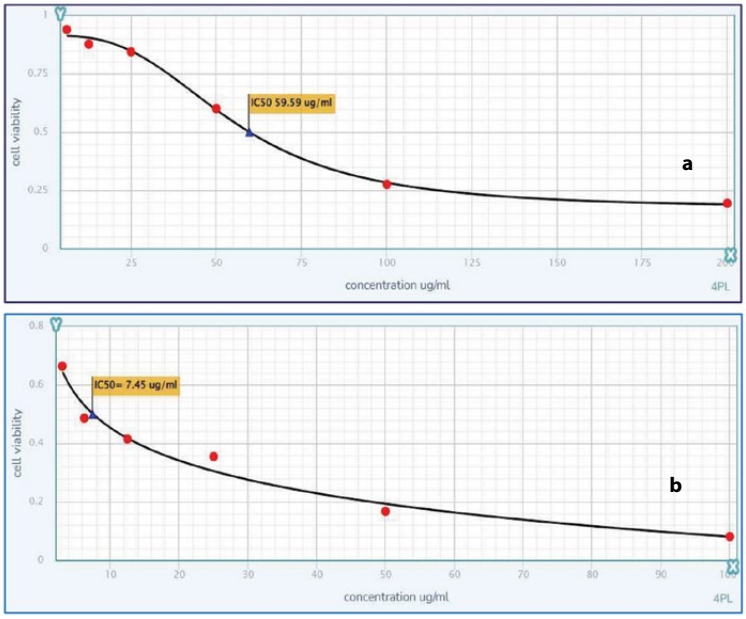

Fig. 10. Computing IC50 values using fractional cells in GraphPad Prism 6. The concentration at which the curve crosses the 50% inhibition threshold is known as the IC50 (a) MFC-7 cells treated with LuAgNPs for 24 h; (b) MFC-7 cells treated with standard luteolin

■ CONCLUSION

Under optimal circumstances of 70 °C and pH 7, LU-AgNPs were generated employing isolation luteolin as a reducing and capping agent. Using UV-VIS, FTIR, XRD, and SEM methods, these synthesized LU-AgNPs were examined. The spherical form of LU-AgNPs revealed a typical particle size of 65.79 nm. According to the antibacterial tests, LU-AgNPs

shows promising antibacterial activity against both Gram-positive and Gram-negative bacteria. The anti-cancer activity for LU-AgNPs was significantly higher than that of free Luteolin with IC50 value 7.45 g/l.

■ REFERENCES

1. Thapliyal A., Chandra A. Antibacterial and anticancer potential of silver nanoparticles synthesized using gallic acid in bentonite/starch bio-nanocomposites. *International Journal of Applied Pharmaceutics.* 2018:178–89.
2. Abdul-Karim E.K., Hussein H.Z. The biosynthesis of nanoparticles by fungi and the role of nanoparticles in resisting of pathogenic fungi to plants: a review. *Basrah Journal of Agricultural Sciences.* 2022;35(1):243–56.
3. Keerthiga N., Anitha R., Rajeshkumar S., Lakshmi T. Antioxidant activity of cumin oil mediated silver nanoparticles. *Pharmacognosy Journal*. 2019;11(4).
4. Almohammed H.I., Albalawi A.E., Al Sadoun H., Bakhtiari N., Amraei M., Moghaddam A., et al. Applying nanoparticles for treating giardia infection: a systematic review. *International Journal of Applied Pharmaceutics.* 2021;13(5):15–9.
5. NW Ali Z., BA Alabdulaziz M. Green Synthesis of Cobalt Nanoparticles and their Application in Removal of Lead from Polluted Water. *Basrah Journal of Science.* 2021;39(2):292–305.
6. Sangour M.H., Ali I.M., Atwan Z.W., Al Ali A.A.A.L.A. Effect of Ag nanoparticles on viability of MCF-7 and Vero cell lines and gene expression of apoptotic genes. *Egyptian Journal of Medical Human Genetics.* 2021;22:1–11.
7. Caio H., Barros I., Fulaz S., Stanisic D., Tasic L. Biogenic nanosilver against multidrug-resistant bacteria (MDRB) antibiotics. *Antiobiotics.* 2018;7:69.
8. Al-Mudhafar S., Al-Hamdani M.A. Evaluation for antibacterial and antiproliferative activity against cancer cell lines of biosynthesized silver nanoparticles from Vitex Agnus-Castus and Uncaria Tomentosa extracts. *Journal of Basrah Researches ((Sciences)).* 2021;47(1).
9. Al-Musawi Z.F., Al-Saadi N.H. Antitumor activities of biosynthesized silver nanoparticles using Dodonaea viscosa (L.) leaves extract. *Basrah Journal of Agricultural Sciences.* 2021;34(2):42–59.
10. Ramírez-Rosas S.L., Delgado-Alvarado E., Sanchez-Vargas L.O., Herrera-May A.L., Peña-Juarez M.G., Gonzalez-Calderon J.A. Green Route to Produce Silver Nanoparticles Using the Bioactive Flavonoid Quercetin as a Reducing Agent and Food Anti-Caking Agents as Stabilizers. *Nanomaterials.* 2022;12(19):3545.
11. Raut R.W., Mendhulkar V.D., Kashid S.B. Photosensitized synthesis of silver nanoparticles using Withania somnifera leaf powder and silver nitrate. *Journal of Photochemistry and Photobiology B: Biology.* 2014;132:45–55.
12. Khan M., Khan M., Adil S.F., Tahir M.N., Tremel W., Alkhathlan H.Z., et al. Green synthesis of silver nanoparticles mediated by Pulicaria glutinosa extract. I*nternational journal of nanomedicine.* 2013:1507–16.
13. Huq M.A. Green synthesis of silver nanoparticles using Pseudoduganella eburnea MAHUQ-39 and their antimicrobial mechanisms investigation against drug resistant human pathogens. *International journal of molecular sciences.* 2020;21(4):1510.
14. Aydoğmuş-Öztürk F., Jahan H., Beyazit N., Günaydın K., Choudhary M.I. The anticancer activity of visnagin, isolated from Ammi visnaga L., against the human malignant melanoma cell lines, HT 144. *Molecular biology reports.* 2019;46:1709–14.
15. Mat Yusuf S.N.A., Che Mood C.N.A., Ahmad N.H., Sandai D., Lee C.K., Lim V. Optimization of biogenic synthesis of silver nanoparticles from flavonoid-rich Clinacanthus nutans leaf and stem aqueous extracts. *Royal Society open science.* 2020;7(7):200065.
16. Kharat S.N., Mendhulkar V.D. Synthesis, characterization and studies on antioxidant activity of silver nanoparticles using Elephantopus scaber leaf extract. *Materials Science and Engineering: C.* 2016;62:719–24.
17. Lokina S., Stephen A., Kaviyarasan V., Arulvasu C., Narayanan V. Cytotoxicity and antimicrobial activities of green synthesized silver nanoparticles. *European journal of medicinal chemistry.* 2014;76:256–63.
18. Kanipandian N., Thirumurugan R. A feasible approach to phyto-mediated synthesis of silver nanoparticles using industrial crop Gossypium hirsutum (cotton) extract as stabilizing agent and assessment of its in vitro biomedical potential. *Industrial Crops and Products.* 2014;55:1–10.
19. Lin P-C., Lin S., Wang P.C., Sridhar R. Techniques for physicochemical characterization of nanomaterials. *Biotechnology advances.* 2014;32(4): 711–26.
20. Murdock R.C., Braydich-Stolle L., Schrand A.M., Schlager J.J., Hussain S.M. Characterization of nanomaterial dispersion in solution prior to in vitro exposure using dynamic light scattering technique. *Toxicological sciences*. 2008;101(2):239–53.
21. Waseda Y., Matsubara E., Shinoda K. *X-ray diffraction crystallography: introduction, examples and solved problems.* Springer Science & Business Media; 2011.
22. Bar H., Bhui D.K., Sahoo G.P., Sarkar P., De S.P., Misra A. Green synthesis of silver nanoparticles using latex of Jatropha curcas. *Colloids and surfaces A: Physicochemical and engineering aspects.* 2009;339(1–3):134–9.
23. Sidjui L., Ponnanikajamideen M., Malini M., Famen L., Sindhu R., Chandirika J.U., et al. Lovoa trichilioides root back mediated green synthesis of silver nanoparticles and rating of its antioxidant and antibacterial activity against clinical pathogens. *Journal of Nanoscience and Technology.* 2015:32–6.
24. Begum N., MH M.I., Mathew S., Govindaraju A., Qadri I. Green synthesis, antioxidant potential and hypoglycemic effect of silver nanoparticles using Ethanolic leaf extract of Clausena anisata (Willd.) Hook. F. Ex Benth. of Rutaceae. *Pharmacognosy Journal.* 2016;8(6).
25. Fissan H., Ristig S., Kaminski H., Asbach C., Epple M. Comparison of different characterization methods for nanoparticle dispersions before and after aerosolization. *Analytical Methods.* 2014;6(18):7324–34.
26. Bhakya S., Muthukrishnan S., Sukumaran M., Muthukumar M. Biogenic synthesis of silver nanoparticles and their antioxidant and antibacterial activity. *Applied Nanoscience.* 2016;6:755–66.
27. Cree I.A. *Cancer cell culture: methods and protocols.* Springer; 2011.
28. Lee S.H., Jun B-H. Silver nanoparticles: synthesis and application for nanomedicine. *International journal of molecular sciences*. 2019;20(4):865.